

Progress in Two Dimensional Arrays for Real Time Volumetric Imaging

E. D. Light, R. E. Davidsen, J.O. Fiering, T. A. Hruschka, S. W. Smith

Department of Biomedical Engineering
Duke University
Durham, NC 27708-0281

The design, fabrication, and evaluation of two dimensional array transducers for real time volumetric imaging are described. The transducers we have previously described operated at frequencies below 3 MHz and were unwieldy to the operator because of the interconnect schemes used in connecting to the transducer handle. Several new transducers have been developed using new connection technology. A $40 \times 40 = 1600$ element 3.5 MHz array was fabricated with 256 transmit and 256 receive elements. A $60 \times 60 = 3600$ element 5.0 MHz array was constructed with 248 transmit and 256 receive elements. An $80 \times 80 = 6400$ element 2.5 MHz array was fabricated with 256 transmit and 208 receive elements. 2-D transducer arrays were also developed for volumetric scanning in an intracardiac catheter, a $10 \times 10 = 100$ element 5.0 MHz forward looking array and an $11 \times 13 = 143$ element 5.0 MHz side scanning array. The -6 dB fractional bandwidths for the different arrays varied from 50% to 63%, and the 50 Ohm insertion loss for all the transducers was about -64 dB. The transducers were used to generate real time volumetric images in phantoms and *in vivo* using the Duke University real time volumetric imaging system which is capable of generating multiple planes at any desired angle and depth within the pyramidal volume.

KEY WORDS: Transducer, two-dimensional array, volumetric imaging

I. INTRODUCTION

The ultrasound transducer is the critical element and the limiting factor in determining the quality of diagnostic ultrasound images and Doppler measurements. Current state of the art clinical scanners typically use linear arrays ($N \times 1$) of more than 100 elements to electronically steer and focus the ultrasound beam. However, these arrays can only produce B-scans with a fixed focus lens in the elevation direction. Thus, at some depths, the lateral resolution in the elevation direction can be many times larger than that in the azimuth direction. This asymmetry of the ultrasound beam can make it very difficult to detect small cysts and lesions in the abdomen, fetus or myocardium. In order to reduce slice thickness, and improve elevation resolution, 1.5D ($N \times M$, $M < 8$) arrays have been proposed and implemented in some systems.^{1,2,4,5,6} These transducers allow for some dynamic focusing in the out of plane dimension, thereby reducing the slice thickness.

Other applications for 1.5D arrays include synthetic aperture imaging and correction of phase aberrations caused by random tissue inhomogeneities. Synthetic aperture techniques make use of multiplexed subapertures of the transducer to improve resolution without increasing the rf channel count of the system. By using 1.5 D arrays, this technique could be used to improve resolution in both the elevation and azimuth directions. Random changes in the velocity in tissue which leads to phase aberration across the front of the transducer can severely reduce image quality. In recent years, it has been shown that these irregularities occur in two dimensions within the body, and require at least a 1.5D array to correct the phase aberrations.³

While 1.5D arrays can be used to reduce the slice thickness in the elevation direction, they cannot steer in the elevation direction, so they are limited to making a single tomographic slice image. These B-mode images can be difficult to obtain in cardiac applications because of the small acoustic windows provided by the ribs. A two dimensional array ($N \times N$) can be steered and/or dynamically focused in both the elevation and azimuth direction. Thus, a pyramidal volume is scanned within the patient⁷⁻⁹ Because a volume of data is created, one can make real time three dimensional scans, which can be used to display any desired plane, including a true short axis of the heart. Applications include the simultaneous display of orthogonal B-scans, acquisition and display of high speed C-scans, display of inclined planes and volumetric, angle independent flow imaging.

Several fabrication methods for constructing two dimensional arrays have been investigated.^{1,10-16} The very large number of elements ($N \times M$) and the difficulty of electrically connecting to the very small elements has limited most 2-D arrays to operating frequencies of approximately 2.5 MHz. For example, a conventional linear phased array consists of 128 operating channels with a $\lambda/2$ interelement spacing in a fully sampled aperture. Interelement spacing at 3.5 MHz would then be 0.2 mm, and the spacing for a 5.0 MHz array would be 0.15 mm. To make similar quality images, a fully sampled two dimensional array would require $(128)^2 = 16,384$ elements. Because of the cost and complexity of building such a large number of rf channels, it is unlikely that anyone will construct such an ultrasound imaging system in the near future. Also, connecting to so many tiny elements in such a dense aperture is very difficult.

In order to reduce the number of channels in the system, undersampling the 2-D array becomes a necessity. Many sparse array designs have been analyzed by several groups.¹⁷⁻²⁰ Approaches that have been pursued are (1) periodic element distribution in which the interelement spacing is different for the transmit and receive apertures in order to reduce grating lobe and side lobe effects^{20,21} and (2) random array geometry¹⁸ with a Gaussian sampling of the transmit aperture and a uniform sampling in receive.¹⁹ Because signal to noise ratio is very important in 2D arrays with such small elements which have high electrical impedance, we chose not to apodize these arrays.

There has also been much interest lately in intravascular ultrasound and intracardiac ultrasound using catheter mounted transducers. Designs include circular side scanning using a rotating single piston transducer²² or a circular array.²³ An alternate approach is a side scanning phased array in a catheter.^{24,25} In addition, there have been some attempts to develop forward looking catheter mounted single element transducers.^{26,27}

In this paper, we will describe the design, fabrication, and test results, including images in tissue mimicking phantoms, of five different two dimensional arrays developed in our laboratory. Each transducer is designed to produce real time three dimensional images using the Duke University volumetric imaging system. The arrays include (1) an $80 \times 80 = 6400$ element array operating at 2.5 MHz for abdominal imaging applications, (2) A $40 \times 40 = 1600$ element array operating at 3.5 MHz for cardiac imaging applications, (3) A $60 \times 60 = 3600$ element array operating at 5.0 MHz for pediatric cardiac imaging applications, (4) A forward looking $10 \times 10 = 100$ element array operating at 5.0 MHz for cardiac catheter applications, and (5) an $11 \times 13 = 143$ element array operating at 5.0 MHz for side scanning cardiac catheter applications. The design characteristics and performance of these transducers will be compared to a control array of $40 \times 40 = 1600$ elements operating at 2.5 MHz for cardiac applications obtained from a commercial supplier.

II. METHODS

Two main criteria dominate the design for 2D arrays: (1) the desired vibration mode of the individual piezoelectric elements, and (2) the characteristics of the ultrasound beam. For 2D arrays, the desired vibration mode is that of a bar in which the length and width are less than the height of the piezoelectric element. The bar is free to move in both the lateral directions, and the resonant frequencies of these modes are above the desired pass band of the transducer. In order to vibrate in the bar mode, the element size, a , must be less than the thickness. The thickness of an element is $.5\lambda_m$ for the speed of sound in the piezoelectric material. In order to reduce grating lobes, the interelement spacing, d , must be less than λ in the propagating medium, in this case, tissue. The two criteria place similar restrictions upon the size of our transducer elements. To model the resonant performance of our 2D array elements, we use the KLM model. To simulate the beam response from the 2D arrays we have designed, we used the software developed by Jensen and Svendsen.²⁸ We, and others, have previously validated the accuracy of these modeling techniques.^{19,28,29} Using the results of these simulations, we determined the array geometry for each desired application.

The volumetric imaging system we use also adds design constraints to the transducers. The system has 256 transmit channels and 256 receive channels for a total of 512 elements. Of these elements, a minimum of 68 and a maximum of 72 must be shared. We typically have 440 possible element locations from which to choose our geometry. This number of elements defines how sparse our arrays will be. In order to fit into the acoustic window between the ribs, a necessity for cardiac scanning, we chose our total array aperture size to be about 12.5 mm. Since the interelement spacing decreases with increasing frequency, the total number of array elements increases with an increase in frequency for a fixed aperture size. Since we are limited in our number of usable elements to 440, a higher frequency transducer will be more sparse than a lower frequency transducer.

Another design constraint of our imaging system is the need for a wide transmit beam width in order to implement the parallel processing technique.^{7,9} To increase the data acquisition rate, we receive 16 receive lines for each transmit line. The receive lines are independently steered in a 4 x 4 matrix around the transmit line. In order for each of the 16 receive lines to process uniform data, the transmit beam width must encompass all the receive lines. This requires that the -6 dB transmit beamwidth be at least 3° . This forces us to concentrate our transmit elements into the center of the array. In order to obtain a useful transmit-receive beam response, we make our receive aperture bigger than the transmit aperture.

A. 40 x 40 2.5 MHz Control Array

Figure 1a shows the simulated transmit receive beam response of the 2.5 MHz 2D control array. This transducer was designed by us, but built by a commercial supplier. It is a $40 \times 40 = 1600$ element array operating at 2.5 MHz. In order to meet the criteria for 2D array elements set above; the interelement spacing, d , is 0.35 mm ($.6\lambda$), the element width and length, a , is 0.30 mm and the thickness, t , is 0.61 mm. The ratio of the width to the thickness is 0.49, which forces the element to operate in the bar mode. The total aperture size is approximately 13 mm, and the transmit and receive elements are in a periodic distribution. This array has been in clinical trials for 2 years, scanning over 200 cardiac patients. Figure 1a shows the simulated pulse-echo beam response for the case where the transmit beam is aligned with the receive beam. We can see that the simulated beam response off axis energy decreases with angle down to -68 dB at $\pm 25^\circ$. The -6 dB beam width is 4° and the -20 dB beam width is 6.5° .

B. 80 x 80 2.5 MHz 2D Array

The control array described was designed for cardiac imaging applications. It has a small footprint to fit into the acoustic window between the ribs. However, this small footprint results in a reduced aperture size. The small aperture results in a wide beam response, which impacts system performance and resolution. This wide beam would have a negative impact on cyst and tumor detection in soft tissues. In order to improve the imaging in soft tissue, such as in abdominal and obstetric applications, we designed an array with a larger aperture.

Figure 1b shows the simulated transmit receive beam response for our 2.5 MHz array. The array size is $80 \times 80 = 6400$ elements operating at 2.5 MHz. The array geometry is random, with a Gaussian sampling for the transmit elements and a uniform sampling for the receive elements. The interelement spacing, d , is 0.35 mm ($.6\lambda$), the element width and length, a , is 0.30 mm and the thickness, t , is 0.61 mm, so it meets the criteria for 2D array elements set above;. The ratio of the width to the thickness is 0.49. The total aperture size is 25 mm. From figure 1b, we see that the simulated pulse-echo beam response has an acoustic clutter pedestal of -42 dB. This higher clutter pedestal than the control is a result of using the random array geometry instead of the periodic distribution. For a random array geometry, the height of the pedestal is related to the number of transmit and receive elements used by :¹⁹

$$\text{Pedestal height} \approx \frac{1}{\sqrt{N_t}} \times \frac{1}{\sqrt{N_r}} ,$$

where N_t is the number of transmit elements and N_r is the number of receive elements in the array. There is an improvement in beam response versus the control array as expected from increasing the aperture size. The -6 dB beam width is 1.6° and the -20 dB beam width is 4.0° . This results in a 60% and 38% improvement, respectively, over the control array.

C. 40 x 40 3.5 MHz 2D Array

In order to improve beam response and resolution for cardiac applications, we designed a 3.5 MHz 2-D array. Figure 1c shows the simulated transmit receive beam response of the chosen pattern for our 3.5 MHz array. The array size is $40 \times 40 = 1600$ elements. In order to meet the criteria for 2D array elements, the interelement spacing, d , is 0.35 mm ($.8\lambda$), the element width and length, a , is 0.25 mm and the thickness, t , is 0.4 mm. The ratio of the width to the thickness is 0.62. The total aperture size is 13 mm, and the transmit and receive elements are in a periodic distribution. From figure 1c, we see that the simulated pulse-echo beam response has a clutter floor of -68 dB, but the first grating lobe is now visible. Still, the peak of the grating lobe is only at -58 dB. The -6 dB beam width is 2.4° and the -20 dB beam width is 4.5° . These beam widths correspond to a 38% and 31% improvement over the control array, respectively.

D. 60 x 60 5.0 MHz 2D Array

For pediatric and neonatal cardiac applications we designed the transducer to operate at 5.0 MHz. Figure 1d shows the simulated transmit receive beam response of the chosen pattern for our 5.0 MHz array. The array size is $60 \times 60 = 3600$ elements. The interelement spacing, d , is 0.20 mm ($.67\lambda$), the element width and length, a , is 0.17 mm and the thickness, t , is 0.29 mm, yielding a ratio of the width to the thickness of 0.59. The total aperture size is 11 mm, and the transmit and receive elements are in a periodic distribution. Figure 1d shows the simulated pulse-echo beam

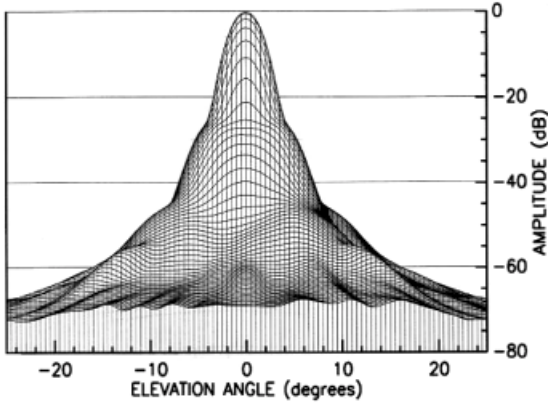


Figure 1a. Simulated transmit receive beam plot of the 2.5 MHz periodic array with 0.35 mm pitch.

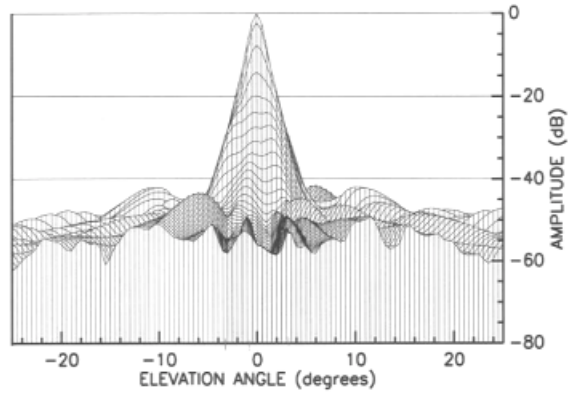


Figure 1b. Simulated transmit receive beam plot of the 2.5 MHz random array with 0.35 mm pitch.

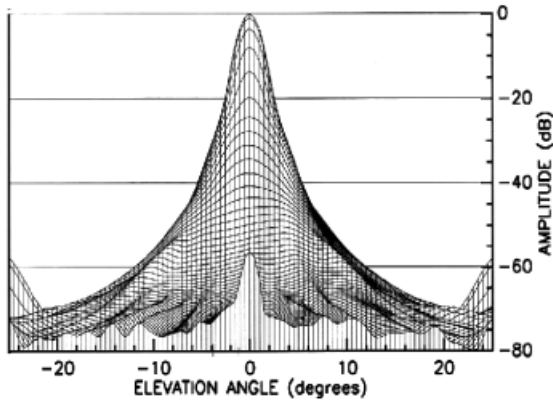


Figure 1c. Simulated transmit receive beam plot of a 3.5 MHz periodic array with 0.35 mm pitch.

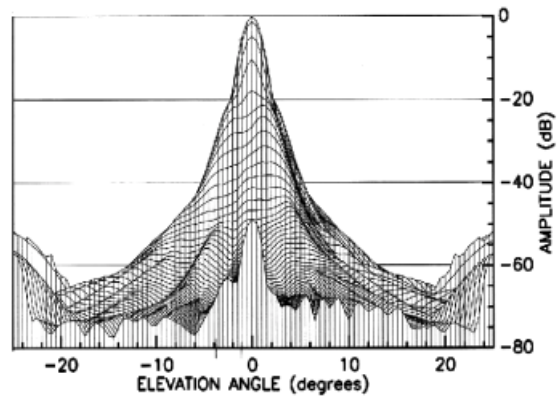


Figure 1d. Simulated transmit receive beam plot of a 5.0 MHz periodic array with 0.20 mm pitch.

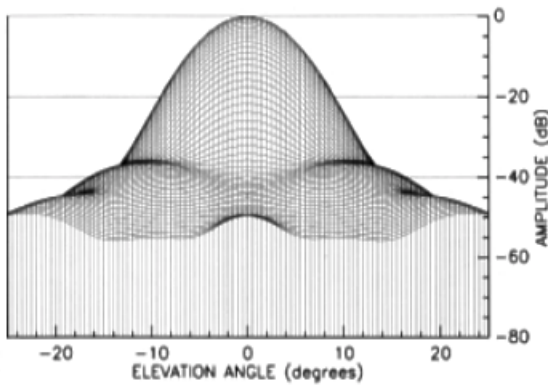


Figure 1e. Simulated transmit receive beam plot of a 10 x 10 5.0 MHz catheter array with 0.20 mm pitch.

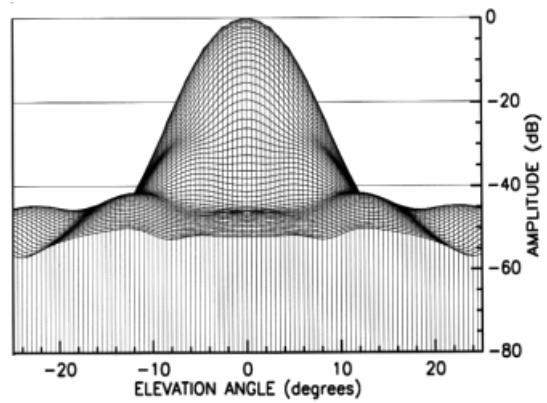


Figure 1f. Simulated transmit receive elevation beam plot of an 11 x 13 5.0 MHz catheter array with 0.20 mm pitch.

response has a clutter floor of -65 dB, but the first grating lobe is now visible. The peak of the grating lobe is only at -52 dB. The -6 dB beam width is 2.2° and the -20 dB beam width is 4.5° . These beam widths correspond to a 45% and 31% improvement over the control array, respectively.

E. 10 x 10 5.0 MHz 2D Array

We have also developed a forward looking 2D array for intracardiac volumetric scanning. Because it is a 2D array, it can focus and/or steer in both the elevation and azimuth dimensions. The array size is $10 \times 10 = 100$ elements, but the corner elements have been removed to approximate a circular aperture. This array uses the same element dimensions as the 60×60 5.0 MHz array to meet the criteria for 2D array elements. There are 71 transmit and 71 receive elements. This array uses the same dimensions as the 60×60 5.0 MHz array to meet the criteria for 2D array elements. The aperture diameter is 2 mm, and the array is fully sampled. In figure 1e, the simulated pulse-echo beam response has a clutter floor of -50 dB. The -6 dB beam width is 10.0° . We pay a considerable price in beam response from the control array, as is expected with an aperture less than one sixth the size of the control array.

F. 11 x 13 5.0 MHz 2D Array

Finally, we have also developed a side scanning 2D array for intracardiac volumetric scanning. The array size is $11 \times 13 = 143$ elements. There are 64 transmit and 64 receive elements. The total aperture size is 3 mm, and the array geometry is periodic. In figure 1f, the simulated pulse-echo beam response has a clutter floor of -50 dB. The -6 dB beam width is 8.0° in the elevation dimension and the -20 dB beam width is 15° in the elevation dimension.

G. Array Fabrication

We have previously described our methods for the fabrication of 2D arrays using epoxy wireguides and pin and socket connectors.^{1,8,29} In order to reduce the size of the handle and make the transducers more usable to medical personnel, the new transducers plug into a convertible cable assembly fabricated by Precision Interconnect (Portland, OR) through seven PI PAC connectors as shown in figure 2. To connect with this handle, we replaced our pin and socket header with 7 polyimide flex circuit connectors. These vertical interconnects are 2 sided, with 36 traces on a side, and have an integrated ground plane in the middle between the two sides. The polyimide circuits also include a fan out from our small transducer footprint to the larger spacing for the PAC connectors. The insulated wires were soldered to these vertical polyimide circuits and then inserted into the wire guide. Table 1 shows the fabrication specifications for each array we constructed.

The 2.5 MHz random array was built on a multi-layer polyimide flex circuit structure made by Litchfield Precision Components (Litchfield, MN). The interelement spacing is $0.35 \text{ mm} \times 0.35 \text{ mm}$. This array used only 6 polyimide flex circuits which were butt soldered vertically onto the back of the multi-layer polyimide flex substrate (MLF). Figure 2 shows a schematic of the transducer fabrication technique, only one vertical interconnect is shown for clarity. Of the 6400 available elements, 392 are connected. We diced the array with a diamond wheel dicing saw (K&S, Willow Grove, PA) mounted with a 0.05 mm blade. We used a 0.10 mm thick Ablefilm conductive epoxy from Ablestick (Rancho Dominguez, CA) as our matching layer. Figure 3

shows a picture of the transducer after dicing. We cast our lossy epoxy onto the back to back fill and add stability to the vertical polyimide connectors.

Table 1. Design specifications for 2D arrays.

Transducer	Interelement spacing (mm)	Array Size	Aperture size (mm)	Number of wired elements	Fabrication Technology
2.5 MHz Control array	0.35	40 x 40	13	440	unknown
2.5 MHz Random array	0.35	80 x 80	25	392	Multi-layer polyimide
3.5 MHz array	0.35	40 x 40	13	440	Drilled epoxy
5.0 MHz array	0.20	60 x 60	11	440	Laser drilled polyimide
5.0 MHz Forward Looking catheter	0.20	10 x 10	2	70	Laser drilled polyimide
5.0 MHz Side Scanning catheter	0.20	13 x 11	3	64	Multi-layer polyimide

For the 3.5 MHz array, the wire guide consisted of a lossy epoxy. We drilled the holes with a Techno-Isel (New Hyde Park, NY) CNC milling machine using a 0.15 mm drill bit. The diamond wheel dicing saw used a 0.10 mm blade, and the matching layer was 0.075 mm thick Ablefilm. The corners were cut off the array to minimize the size of the foot print. Figure 4 shows the array after dicing. The transducer was then put into an aluminum shell, and back filled with more lossy epoxy.

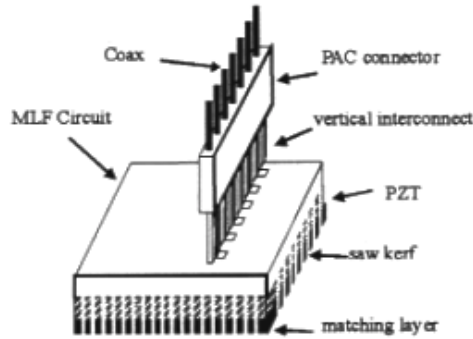


Figure 2. Schematic of the construction technique for the 2.5 MHz random array.

For the 60 x 60 5.0 MHz array, the wireguide was made from laminating pieces of polyimide together. Because of the small hole size required for this transducer, we had the polyimide laser drilled with 0.10 mm holes. We used the same dicing saw as for the 3.5 MHz array, but used a 0.025 mm blade instead. We wired 440 of the 3600 available elements, and we used 0.050 mm thick Ablefilm conductive epoxy. Figure 5 shows the array after dicing.

The wire guide for the forward looking 5.0 MHz catheter array was made from laminating pieces of polyimide together. As in the construction of the 60 x 60 5.0 MHz array, we used a laser to drill the 0.10 mm holes in the polyimide. We wired 71 of the 100 available elements, using only a single PI PAC connector and a special handle assembly created by Precision Interconnect that includes 72 coaxial cables inside a 12 French catheter lumen. The corners were cut off after

dicing the array to accurately fix the footprint to fit into a 12 French (3 mm I.D.) catheter. The transducer was then put into a polymer tube and back filled using the same lossy epoxy as used in the construction of the 3.5MHz array. Figure 6 shows the array after dicing.

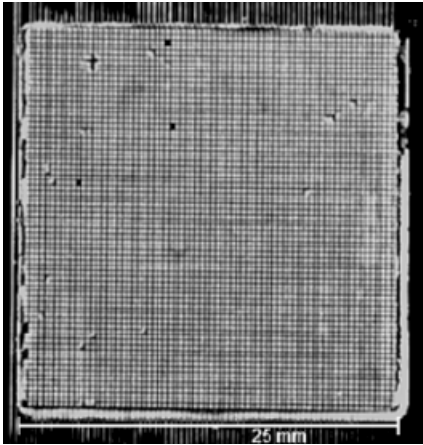


Figure 3. 2.5 MHz random array after Dicing.

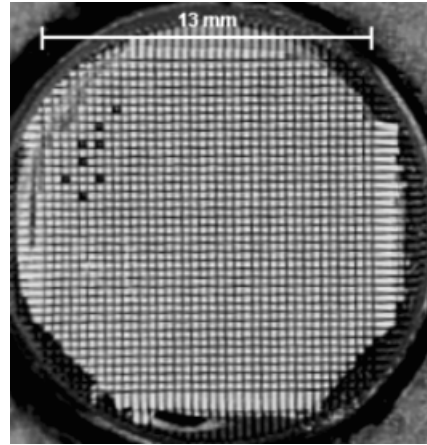


Figure 4. 3.5 MHz array after dicing.

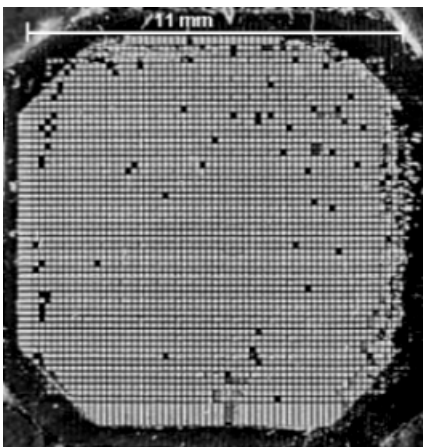


Figure 5. 5.0 MHz array after dicing.

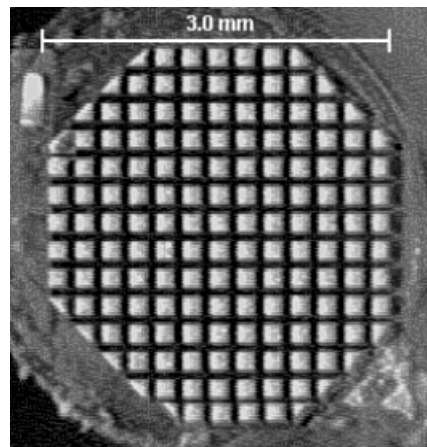


Figure 6. 5.0 MHz 11 x 13 catheter array after dicing.

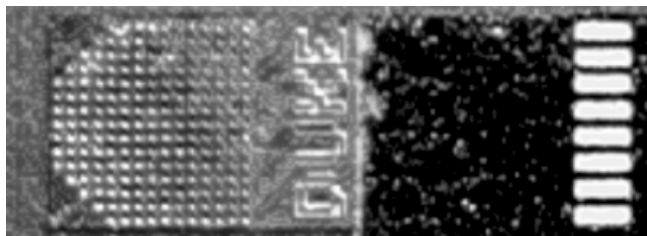


Figure 7. Multi-layer polyimide flex connector for the 11 x 13 side scanning catheter array.

The side scanning 5.0 MHz catheter array was built on a multi-layer polyimide flex circuit made at North Carolina State University (Raleigh, NC) using thin film techniques.¹³ The interelement spacing is 0.20 mm x 0.20 mm. We used the same dicing technique as in the construction of the 60 x 60 5.0 MHz array. We used 0.050 mm thick Ablefilm conductive epoxy from Ablestick as a matching layer. We wired 64 of the 143 available elements, using only 1 PI PAC connector and the assembly described above. Figure 7 shows a picture of the multi-layer flex circuit before

bonding the PZT. The pads for the PZT and the first row of solder pads for the co-axial cables can be seen. After dicing, the transducer was put into a polymer tube and back filled using a silicone adhesive.

H. Performance Testing

To measure the performance of all the 2D arrays, we performed standard tests for single elements for each transducer. These tests were pitch catch sensitivity and bandwidth, 50 Ω insertion loss, angular response, and interelement cross coupling. Pitch catch sensitivity off an aluminum block in a water tank was measured using a Metrotek Model 215 transmitter (20 ns rise time) and a 10 pf Tektronix oscilloscope probe into a Tektronix model TDS 744A Digitizing Oscilloscope. The pitch catch spectrum was measured with a Panametrics 5052G Stepless Gate and a Hewlett-Packard model 3588A Spectrum Analyzer.

To measure the 50 Ω pitch catch insertion loss, we used a Hewlett-Packard model 8165A Programmable Signal Source Generator and an ENI model 325LA RF Power Amplifier with a 50 Ω output impedance to produce a 3 cycle burst at the desired frequency. We attached this to our transmit element. We loaded our receive element by setting the scope probe input impedance to 50 Ω . To minimize losses due to diffraction, we moved our reflector as close as possible to the face of the transducer.

Interelement cross talk decreases the angular response of the individual elements limiting the ability to steer the array. Cross talk measurements were made by transmitting on a single element in the water tank, and measuring the response to the transmit pulse in nearest neighbors. The transducer handle was attached, and each element was loaded with a Tektronix scope probe to simulate the actual in use situation. In each case, the measured signal was received at the same time as the transmitted signal. This indicates that the main source of cross talk is through electrical pick up, not acoustic.

In order to measure the angular response of the individual elements, we centered the element over a broad band point receiver (Dapco Hydrophone). The element was then rotated about its axis while transmitting. The neighboring elements were loaded with Tektronix scope probes. The output of the hydrophone was normalized and squared to calculate pulse echo response.

III. RESULTS

A. Measurement Results

The results from the transducer tests are summarized in Table 2. Figures 8-12 show the pitch-catch pulses and spectra acquired from typical elements in each of the transducer arrays. The sensitivities varied from 4.5 mV_{p-p} to 25 mV_{p-p}. The catheter assemblies are loaded with 3 ft of coaxial cable, so it is natural that their response is lower. The -6 dB fractional bandwidths vary from 50% to 63%. From Table 2, the range of insertion losses is from -63 dB to -69 dB, the angular response varies from 14° to 36°, and the crosstalk is between -26 dB and -32 dB. The tissue penetration ranges from 5.0 cm for the 5.0 MHz array to more than 12 cm for both the 2.5 MHz arrays.

Table 2. Results from transducer testing.

Transducer	Center Frequency (MHz)	-6 dB Fractional Bandwidth	50 Ω Insertion Loss	Cross Talk	-6 dB Angular Response
2.5 MHz Random Array	2.6 MHz	54%	-64 dB	-26 dB	14°
3.5 MHz Array	3.2 MHz	63%	-63 dB	-32 dB	42°
5.0 MHz Array	5.0 MHz	50%	-69 dB	-31 dB	18°
5.0 MHz Catheter Array	5.2 MHz	50%	-64 dB	-26 dB	36°

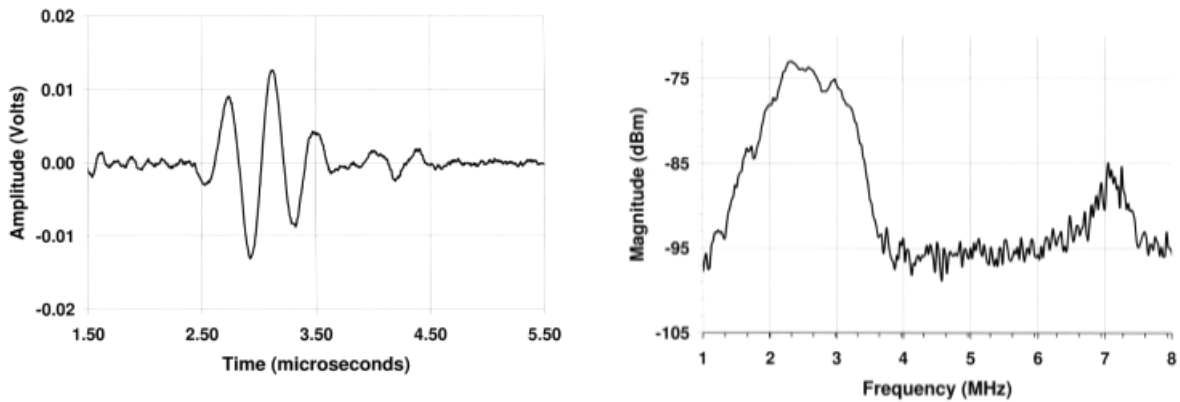


Figure 8. Pitch – catch a) pulse and b) spectrum of 2.5 MHz random array.

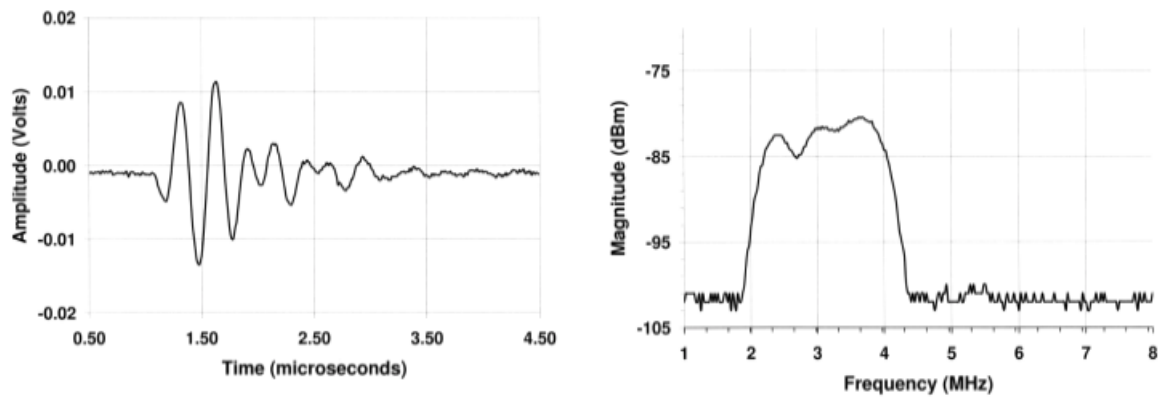


Figure 9. Pitch – catch a) pulse and b) spectrum of 3.5 MHz array.

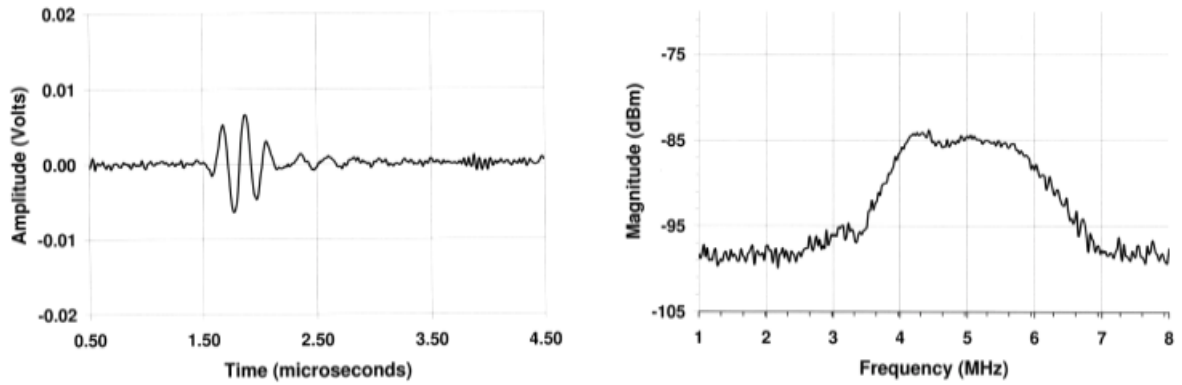


Figure 10. Pitch – catch a) pulse and b) spectrum of 5.0 MHz array.

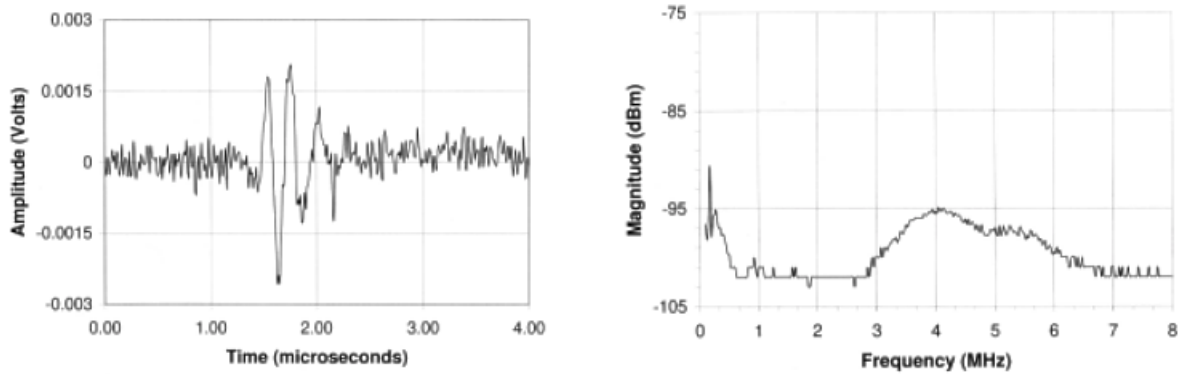


Figure 11. Pitch – catch a) pulse and b) spectrum of 5.0 MHz 10 x 10 catheter array.

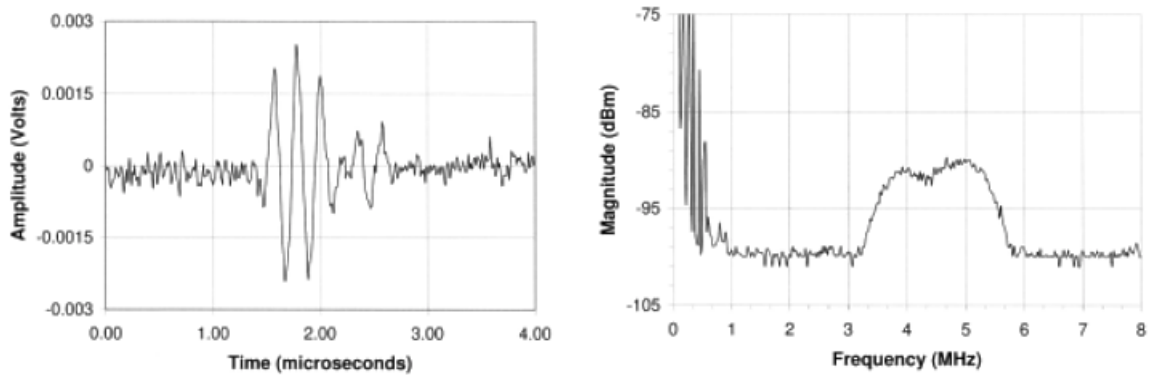


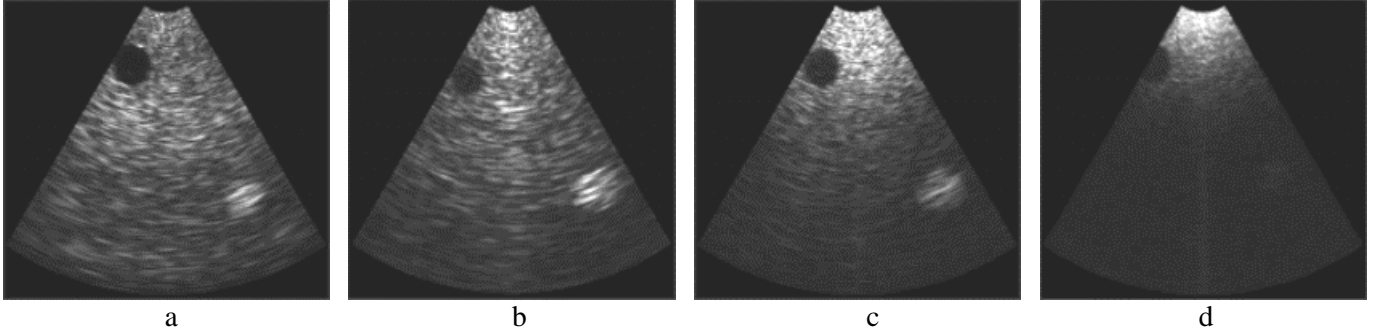
Figure 12. Pitch – catch a) pulse and b) spectrum of 5.0 MHz 11 x 13 catheter array.

B. Images

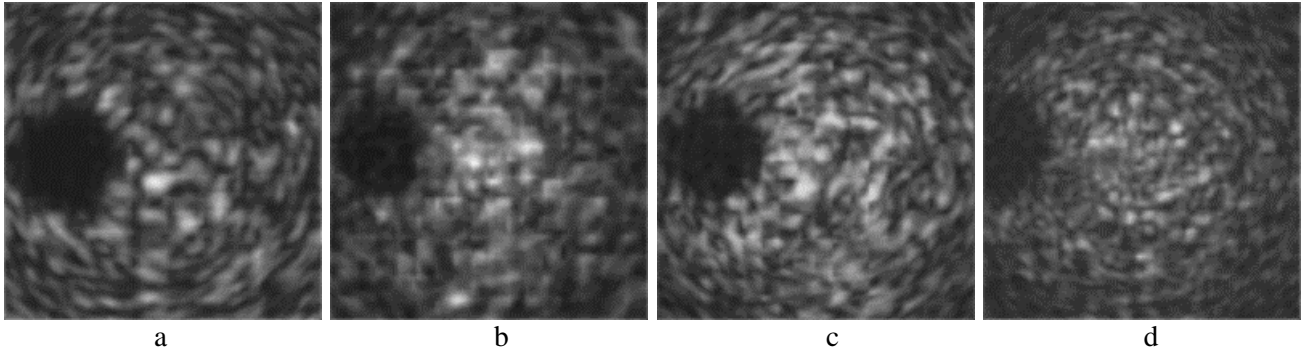
Figures 13 – 17 show typical images obtained with the Duke volumetric scanner in tissue mimicking phantoms. Figure 13 shows a typical B-scan through a phantom that includes a fluid filled spherical cyst at the top and a solid lesion near the bottom. Each target is 10 mm in diameter. The scan depth for each image is 14 cm. The phantom has an attenuation of approximately .5dB/cm-MHz. Receive mode gain was adjusted to optimize each of the images at

the time of scanning. Figure 14 shows the perpendicular real time C-scan parallel to the transducer face through the cyst in figure 13.

Figures 13a and 14a were taken with the 2.5 MHz commercial array. The images show a uniform angular response and contrast resolution with little cyst fill-in.



Figures 13a, 13b, 13c and 13d. B-Mode phantom images using a) the 2.5MHz commercial array, b) the 2.5 MHz random array, c) the 3.5 MHz array and d) the 5.0 MHz array.



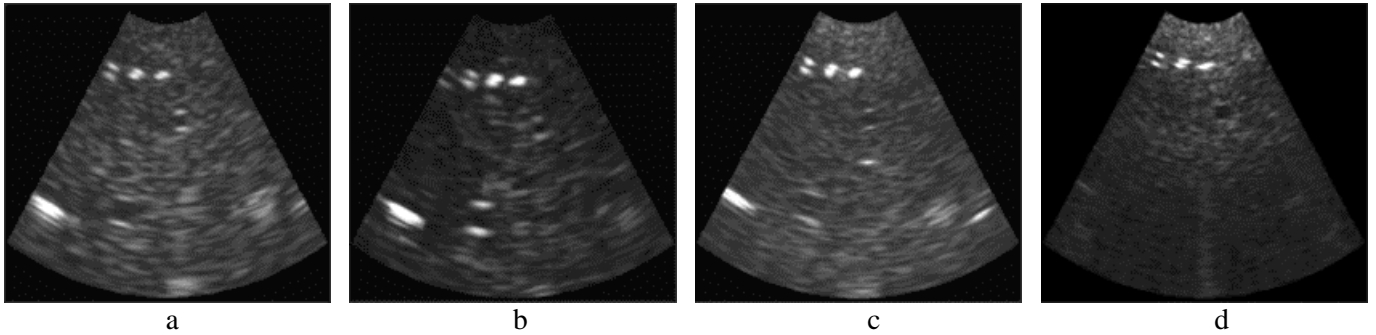
Figures 14a, 14b, 14c and 14d. C-modes slices through the phantom used in figure 13 with a) the 2.5 MHz commercial array, b) the 2.5 MHz random array, c) the 3.5 MHz array and d) the 5.0 MHz array.

Figures 13b and 14b show the same phantom using the 2.5 MHz random array. These image show a reduction in speckle size from the commercial transducer as expected from the larger aperture and the simulated beam plot of figure 1b. The higher sidelobe floor in the beam seen in figure 1b leads to more cyst fill-in than the commercial array. There is also an image artifact since the transmit beam is too narrow for our receive parallel processing technique. This causes the blocky appearances in the C-scan.

Figures 13c and 13d show the same phantom with the 3.5MHz and 5.0 MHz arrays respectively. The improvement in resolution can be seen in the finer speckle size versus the 2.5 MHz commercial array. This is also seen in the C-scans of figures 14c and 14d. It is also clear in figure 13d that the 3.5 MHz and 5.0 MHz arrays have less penetration in the phantom than the lower frequency arrays. The 3.5 MHz array penetrates to 11 cm and the 5.0 MHz array only penetrates to 5.0 cm. This is expected since the phantom has frequency dependent attenuation, and the 5.0 MHz array has a smaller footprint than the other transducers. Also, both the 3.5 MHz and the 5.0 MHz transducer images show cyst fill-in. These arrays do not have as good a signal to noise ratio as the control array. Also, looking at figures 1c and 1d, the beam profiles of these arrays have grating lobes at 25° off axis. These grating lobes will add to the cyst fill-in because

in order to get a B-scan that included both the cyst and the deeper tumor, the cyst was positioned near the edge of the sector scan.

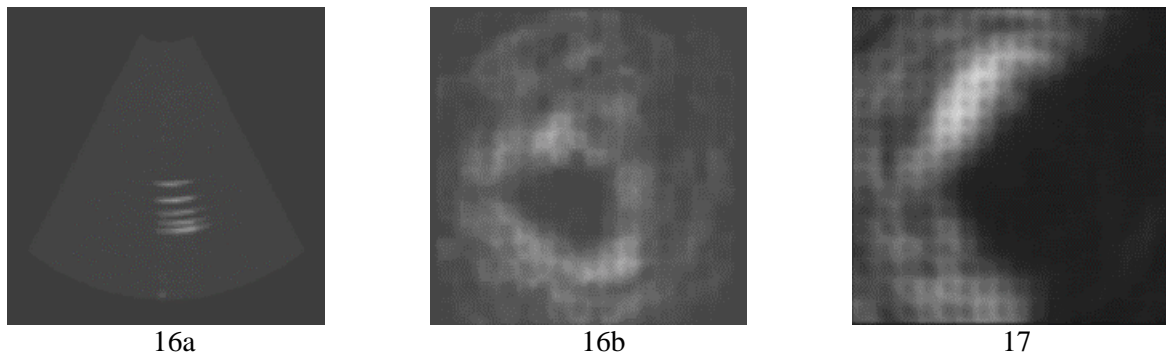
Figure 15 shows typical B-mode images made in a CIRS Model 40 phantom (Norfolk, VA) that includes axial resolution targets as well as two fluid filled cysts in the region of interest. The attenuation is 0.5 dB/cm-MHz. The depth of scan is 8 cm in each case, and the images have been optimized for each transducer. Figure 15a was taken with the 2.5 MHz commercial transducer.



Figures 15a, 15b, 15c, 15d. B-mode images from the CIRS phantom using a) the 2.5 MHz commercial array, b) the 2.5 MHz random array, c) the 3.5 MHz array and d) the 5.0 MHz array.

Figure 15b shows the same phantom using the 2.5 MHz random array. The speckle is finer and the deep cyst qualitatively seems better resolved.

Figures 15c and 15d show the same phantom using the 3.5 MHz and 5.0 MHz transducers, respectively. In each image, the strings are sharper laterally and the speckle is finer compared to the 2.5 MHz commercial array. The 5.0 MHz array also shows axial resolution improvement with the string targets. In both figures, it is easier to detect the near cyst than with either of the 2.5 MHz arrays, with the 5.0 MHz image being the best. The specular reflection in the cyst is reduced in the case of the 3.5 MHz array, and practically nonexistent with the 5.0 MHz transducer. Again we see that the 5.0 MHz transducer has reduced penetration due to frequency dependent attenuation, while the 3.5 MHz array has similar penetration to the two 2.5 MHz transducers at the displayed depth of scan.



Figures 16a, 16b. Images made with the 5.0 MHz forward looking catheter transducer, a) B- scan of strings in a water tank, b) C-scan of a 11.5 mm diameter hole in a sponge. Figure 17. A C-scan of a hole in a sponge made with the 5.0 MHz side scanning catheter transducer.

Figure 16 shows the images made with the 5.0 MHz forward looking catheter array. Figure 16a shows the AIUM axial resolution targets in a water tank, the depth of scan is 8 cm. The six

strings are spaced 5, 4, 3, 2, and 1mm apart, but we only resolve five. Figure 16b shows a C-scan through a sponge with an irregular hole cut in it to simulate a face on views of a cardiac valve. The hole in the sponge for figure 16b is 11.5 mm in diameter. Even though the beam is quite wide, we can clearly see this change in diameter. Figure 17 shows a C-scan made with the side scanning catheter of a right angle notch in the edge of the sponge.

IV. DISCUSSION

We have described the design, fabrication and performance testing of several 2D array transducers for real time volumetric imaging. We have overcome several challenges in the design and fabrication of higher frequency 2D arrays. We have previously stated that we would not be able to overcome the limitation of hand wiring techniques to produce 2D transducer arrays operating at frequencies above 3 MHz.¹ With the research in sparse arrays combined with the availability of laser drilling and thinner wire, we have been able to develop 5.0 MHz 2D arrays. An 80 x 80 2.5 MHz array was developed to improve abdominal volumetric images over the images generated by the cardiac 2D arrays available. Once we received the multi-layer polyimide substrate, this transducer was built in less than a week, compared to three weeks for both the 40 x 40 3.5 MHz array and 60 x 60 5.0 MHz array. This improvement in fabrication time should be a valuable asset in the large scale production of two-dimensional arrays. Unfortunately, the amount of time it takes to receive multi-layer polyimide substrates is usually over 8 weeks, if it can be done at all. While this amount of time is acceptable for production runs of many similar transducers, it does not lend itself well for research prototyping.

Several other researchers have also fabricated multi-dimensional arrays with measurement results similar to those in this paper, but to the best of our knowledge, none have shown any pulse echo images. The literature reports 1.5 D arrays operating up to 3.5 MHz with -6 dB fractional bandwidths around 70%.^{4,5} 2D arrays operating between 2.5 MHz and 3.2 MHz with bandwidths ranging from 30% to 50% are reported.^{14,15,16} These 2D arrays also have similar angular response and cross talk to the arrays reported here.^{14,15}

As we can see from Table 2, there is a variance in the measured -6 dB fractional bandwidth from 50% to 63%. By using the Ablefilm material as a matching layer we limited ourselves to the available thickness' of the Ablefilm. The material is soft, and cannot be machined. The ratios of the different thickness' of the Ablefilm do not correspond to the ratios of the different frequencies of the transducer arrays. Also, the material will deform under the pressure of bonding. This makes it difficult during the fabrication of the catheter arrays. These transducers have a small area, so bonding pressures are higher than for the larger arrays.

Both the 3.5 MHz and the 5.0 MHz transducers demonstrated less penetration than the control array in the phantom images. Each phantom has frequency dependent attenuation which will greatly affect the return signal as frequency increases. To further decrease its penetration, the 5.0 MHz array has about 10% dead elements, a smaller aperture, and 6 dB worse insertion loss than the 3.5 MHz array. The dead elements are due to difficulties in the fabrication of this first 5.0 MHz 2D array.

The interelement crosstalk for the arrays shown in Table 2 is worse than we would prefer. For the random array, the main source of cross coupling is the polyimide flex circuits attached to the transducers. These flex circuits do have a ground plane between the two sides of the board, but do not have a ground trace between each signal trace. For the 3.5 MHz and the 5.0 MHz arrays, the main source of crosstalk is the unshielded wires in the wireguide.

Images of tissue mimicking phantoms with the 40 x 40 3.5 MHz array and 60 x 60 5.0 MHz array both demonstrated improved resolution over the control array. Initial cardiac scanning in both the adult and pediatric population also shows improved volumetric images over the control array. Both transducers are now in clinical trials.

A 10 x 10 5.0 MHz catheter array was developed for forward viewing intracardiac volumetric images. With this transducer, we have made images of tissue mimicking phantoms, including dynamic cardiac valve studies. We have also made phantom images with an 11 x 13 5.0 MHz side viewing catheter array. These arrays represent exciting prospects for intracardiac diagnosis and therapy, and also the possibility for minimally invasive breast imaging with biopsy needles.

There are still more challenges to overcome. We will need to improve our matching layer scheme to increase the bandwidth of the 2D arrays. We will also need higher frequency 2D arrays. We believe it is feasible to make a 2D array operating at 7.5 MHz with the current methods. In order to go to arrays of higher frequencies, the arrays will need to be more sparse, and the hole sizes will need to be smaller. The technology does exist, but going to laser drilled holes below 0.1 mm in diameter, requires the use of more expensive lasers and will increase the cost of the fabrication.

For volumetric imaging to become a useful diagnostic tool, it must be able to offer all the capabilities of a current B-mode imaging system. This includes many transducer arrays operating at several frequencies. We have demonstrated that 2D arrays operating at frequencies above 2.5 MHz can be fabricated and that they offer the same advantages that higher frequency 1D arrays have over lower frequency 1D arrays. However, more research into better matching layers and piezoelectric materials such as single crystals³⁰ and multi-layer PZT²⁹ is needed if we are to have 2D arrays with similar bandwidth and insertion loss of 1D arrays.

V. REFERENCES

1. Smith, S. W., Trahey, G. E., and von Ramm, O. T., "Two-Dimensional arrays for medical ultrasound", *Ultrasonic Imaging*, vol. 14, pp. 213-233, 1992.
2. Smith, L. S., Engler, W. E., O'Donnell, M. and Piel, J. E., Jr., "Rectilinear phased array using 2-2 ceramic polymer composite", *Proceedings of the IEEE Ultrasonics Symposium*, 90CH2938-9, pp. 805-808, 1990.
3. Trahey, G. E., LeBlanc, B. H., Kaebler, D. C. and Freiburger, P. D., "The necessity of two-dimensional phased array for successful phase aberration correction", *Ultrason. Imag.* vol. 13, pp. 197-198 (1991).
4. Tournois, P., Calisti, s., Doisy, Y., Bureau, J. M. and Bernard, F., "A 128x4 channels 1.5D curved linear array for medical imaging", *Proceedings of the IEEE Ultrasonics Symposium*, 95CH35844, pp. 1331-1335, 1995.
5. Zhang, J., Xue, Q. and Ogawa, S., "1.5 Dimensional arrays for effective dynamic focusing and receiving," *Proceedings of the IEEE Ultrasonics Symposium*, 96CH35993, pp. 1531-1534, 1996.
6. Wildes, D.G., Chiao, R.Y., Daft, C.M.W., Rigby, K.W., Smith L.S. and Thomenius, K.E., "Elevation performance of 1.25D and 1.5D transducer arrays," *IEEE Trans. Ultras. Ferro. and Freq. Control*, vol. 44, pp. 1027-1037, 1997.

7. von Ramm, O. T. and Smith, S. W., "Real time volumetric ultrasound imaging system", *Proc. SPIE Symp. Med. Imag. IV*, pp. 15-22, 1990.
8. Smith, S. W., Pavy, H. E. and von Ramm, O. T., "High speed ultrasound volumetric imaging system part I: transducer design and beam steering", *IEEE Trans. Ultras. Ferro. and Freq. Control*, vol. 38, pp. 100-108, 1991.
9. von Ramm, O. T., Smith, S. W. and Pavy, H. E., "High speed ultrasound volumetric imaging system part II: parallel processing and display", *IEEE Trans. Ultras. Ferro. and Freq. Control*, vol. 38, pp. 109-115, 1991.
10. Plummer, J. D., Swartz, R. G., Maginness, M., Beaudouin, J. R. and Meindl, J. D., "Two-Dimensional transmit/receive piezoelectric arrays: construction and performance", *IEEE Trans. on Sonics and Ultrasonics*, vol. 25, pp. 273-280, 1978.
11. Smith, S. W. and Light, E. D., "Two-dimensional array transducers using thick film connection technology", *IEEE Trans. Ultrason. Ferro. and Freq. Control*, vol. 40, pp. 727-734, 1993.
12. Davidsen, R. E. and Smith, S. W., "A multiplexed two-dimensional array for real time volumetric and B-mode imaging", *Proceedings of the IEEE Ultrasonics Symposium*, 96CH35993, pp. 1523-1526, 1996.
13. Davidsen, R.E. and Smith, S.W., "Two-dimensional arrays for medical ultrasound using multi-layer flexible circuit interconnection", *IEEE Trans. Ultrason. Ferro. and Freq. Control*, vol. 45, pp. 338-348, 1998.
14. Greenstein, M., Lum, P., Yoshida, H. and Seyed-Bolorforosh, M.S., "A 2.5 MHz 2D array with z-axis electrically conductive backing", *IEEE Trans. Ultrason. Ferro. and Freq. Control*, vol. 44, pp. 970-977, 1997.
15. Granz, M. B. and Oppelt, R., "A 2-d acoustic array for diagnostic imaging", *Proceedings of the IEEE Ultrasonics Symposium*, 96CH35993, 1573-1576, 1996.
16. Erikson, K., Hairston, A., Nicoli, A., Stockwell, J. and White, T., "A 128 x 128 Ultrasonic Transducer Hybrid Array", *Proceedings of the IEEE Ultrasonics Symposium*, 97CH36118, pp. 1625-1629, 1997.
17. Weber, P. K., Schimdt, R. M., Tylkowski, B. D. and Steck, J., "Optimization of random sparse 2-D transducer arrays for 3-D electronic beam steering and focusing", *Proceedings of the IEEE Ultrasonics Symposium*, 94CH3468-6, pp. 1503-1506, 1994.
18. Turnbull, D. H. & Foster, F. S., "Simulation of B-scan images from two-dimensional transducer arrays: part II- comparisons between linear and two-dimensional phased arrays", *Ultrason. Imag.* vol. 14, pp. 344-353, 1992.
19. Davidsen, R. E., Jensen, J. A. & Smith, S. W., "Two-dimensional random arrays for real time volumetric imaging", *Ultrason. Imag.* vol. 16, pp. 143-163 1994.

20. Brunke S. S. and Lockwood, G. R., "Broad-bandwidth radiation patterns of sparse two-dimensional vernier arrays", *IEEE Trans. Ultrason. Ferro. and Freq. Control*, vol. 44, pp. 1101-1109, 1997.
21. von Ramm, O. T., Smith S. W. and Thurstone, F. L., "Grey scale imaging with complex TGC and transducer array", *Proc. Soc. Photo-opt Inst. Engineers, Medicine IV*, 70, pp. 266-270, 1975.
22. Yock, E.L., Johnson et al. "Intravascular ultrasound: development and clinical potential", *Am J. Cardiac Imaging*, 2, pp. 185-193, 1988.
23. Bom, N., Lancee, C. T. and Van Egmond, F. C., "An ultrasonic intracardiac scanner", *Ultrasonics*, 10, pp. 72-776, 1972.
24. Piel, J. E., Jr. et al., "7.5 MHz pediatric phased array transesophageal endoscope", *Proceedings of the IEEE Ultrasonics Symposium*, 94CH3468-6, pp. 1527-1530, 1994.
25. Seward, J. B., Packer, D. L., Chan, R. C., Curley, M. C. and Tajik, A. J., "Ultrasound Cardioscopy: embarking on a new journey", *Mayo Clinic proceedings*, 71, pp. 629-635, 1996.
26. Evans, J. L., Yock, P. G. et al., "Arterial imaging with a new forward viewing intravascular ultrasound catheter, I initial studies", *Circulation*, 89, pp. 712-723, 1994.
27. Liang, D. H. and Hu, B. S., "A forward viewing intravascular ultrasound catheter suitable for intracoronary use", *Biomed. Instr. And Tech.*, pp. 45 -53, January, 1997.
28. Jensen, J. A. and Svendsen, N. B., "Calculation of pressure fields from arbitrarily shaped, apodized, and excited ultrasound transducers", *IEEE Trans. Ultrason. Ferro. and Freq. Control*, vol. 39, pp. 262-267, 1992.
29. Goldberg, R.L. and Smith, S.W., "Multilayer piezoelectric ceramics for two-dimensional array transducers," *IEEE Trans. Ultrason. Ferro. and Freq. Control*, vol. 41, pp. 761-771, 1994.
30. Lopath, P.D., Park, S., Shung, K.K. and Shrout, T.R., "Single crystal $\text{Pb}(\text{Zn}_{1/3}\text{Nb}_{2/3})\text{O}_3/\text{PbTiO}_3$ (PZN/PT) in medical ultrasound transducers", *Proceedings of the IEEE Ultrasonic Symposium*, 97CH36118, pp. 1643-1647, 1997.